Dry Sliding Wear Behavior of Al 2219/SiCp-Gr Hybrid Metal Matrix Composites

S. Basavarajappa, G. Chandramohan, K. Mukund, M. Ashwin, and M. Prabu

The dry sliding wear behavior of Al 2219 alloy and Al 2219/SiCp/Gr hybrid composites are investigated under similar conditions. The composites are fabricated using the liquid metallurgy technique. The dry sliding wear test is carried out for sliding speeds up to 6 m/s and for normal loads up to 60 N using a pin on disc apparatus. It is found that the addition of SiCp and graphite reinforcements increases the wear resistance of the composites. The wear rate decreases with the increase in SiCp reinforcement content. As speed increases, the wear rate decreases initially and then increases. The wear rate increases with the increase in load. Scanning electron microscopy micrographs of the worn surface are used to predict the nature of the wear mechanism. Abrasion is the principle wear mechanism for the composites at low sliding speeds and loads. At higher loads, the wear mechanism changes to delamination.

1. Introduction

Aluminum metal matrix composites (AMMC) have emerged as a material for advanced automobile and aerospace applications. It possesses properties like high specific strength and modulus, high stiffness, increased fatigue resistance, good wear resistance at elevated temperatures, excellent corrosion resistance, and high temperature durability, etc. (Ref 1-3). These composites are attractive and viable alternatives to the traditional engineering alloys. The suitability of MMCs as a promising replacement depends on the ability of synthesizing them with consistent reproducibility in microstructure and properties. These newer generation materials have an increased power-to-weight ratio. They can be used in automobile applications like brake rotors, piston rings, etc. (Ref 4-7).

Wear performance of discontinuously reinforced metal matrix composites (DRMMC) reinforced with SiCp particle is reported by various researchers. During the dry sliding test of Al/SiCp, Straffelini et al. (Ref 8) found that at loads below 200 N, wear is by abrasion. Riahi and Alpas (Ref 9) found that a tribo-layer is formed during the dry sliding wear test of A356/4SiCp composite. As speed and load increases, the proportion of contact layer covered by the tribolayer increases. Ma et al. (Ref 10) are under the opinion that at high sliding speeds, 50% SiCp reinforced composite exhibits lower wear rates compared with 20% SiCp reinforced composite and unreinforced A390 alloy. Kasim et al. (Ref 11) reported that the abrasive wear resistance of the alloy is increased as SiCp reinforcement content increases. An equally good number of works have been done regarding the wear behavior of graphite-reinforced composites. Seah et al. (Ref 12) reported a drastic increase in the wear resistance of cast ZA-27/Gr composites with the increase

in graphite reinforcement up to 1% (by weight). Further addition of graphite results only in marginal improvement in the wear resistance. The graphite also lowers the hardness of the material. In a dry sliding test of Al/Gr, Mohan et al. (Ref 13) found that graphite smears at the sliding interface and reduces wear, but graphite addition beyond 1.5% reduces the mechanical properties of the composite.

In a majority of the automobile and structural applications, along with an increase in wear resistance, mechanical properties should also increase. The combined effect of aluminum alloy reinforced with ceramics and graphite imparts good wear properties to the composite (Ref 9, 14-16). The coefficient of friction is also lowered due to the lamellar structure and softness of solid lubricants like graphite and MoS_2 (Ref 17). These materials contain a lubricating component that can be released automatically during the wear process. Graphite can be added to retard severe wear at higher temperatures and to delay the onset of seizure (Ref 14). The high seizure resistance is due to the formation of a graphite layer that prevents metal-to-metal contact (Ref 9). In the case of copper matrix composites, incorporation of graphite decreases the wear rate of pin and counterface and prevents the occurrence of severe wear up to 723 K (Ref 14). Riahi and Alpas (Ref 9) reported that transition loads and speeds for graphitic composites are higher when compared with unreinforced A356 and nongraphitic A356/20SiCp composites. In addition, the friction coefficient decreases and becomes more stable as graphite content increases.

An attempt is made in the present work to study the wear behavior of Al 2219 alloy and Al 2219/SiCp/Gr composites. The effect of sliding speed, load, and sliding distance on the wear behavior of the composites is studied. The wear mechanisms are identified at different loads and speeds. The role of graphite in controlling the wear behavior in graphitic composites is discussed in detail.

2. Experimentation

2.1 Materials

Aluminum (AA2219) is used as the base alloy and its chemical composition is given in Table 1 (Ref 18). This matrix

S. Basavarajappa and G. Chandramohan, Department of Mechanical Engineering; and K. Mukund, M. Ashwin, and M. Prabu, Department of Production Engineering, PSG College of Technology, Coimbatore, India-641 004. Contact e-mail: basavarajappas@yahoo.com.

Table 1 Composition of Al 2219 alloy (wt.%)

Element	Weight %
Si	0.20 max
Fe	0.30 max
Cu	5.8-6.8
Mn	0.20-0.40
Mg	0.02 max
Zn	0.10 max
V	0.05-0.15
Ti	0.02-0.1
Zr	0.1-0.25
Al	Balance

is chosen because it provides an excellent combination of strength and damage tolerance at both elevated and cryogenic temperatures. It is an age hardenable alloy suitable for high-temperature and high-strength applications like structural components and high-strength weldments. It has high heat dissipation capacity due to its high thermal conductivity. The four materials Al 2219, Al 2219/5SiCp/3Gr, Al 2219/10SiCp/3Gr, and Al 2219/15SiCp/3Gr are fabricated under similar conditions. The SiCp and graphite of average particle sizes 25 and 45 μm, respectively, are used as reinforcing materials to fabricate the aluminum ceramic graphitic composite.

The liquid metallurgy technique is used to fabricate the composite as it ensures a uniform distribution of the reinforcing particles. This process is similar to the fabrication methods used in earlier research (Ref 19, 20). In this process, the matrix alloy is first superheated above its melting temperature and stirring is initiated to homogenize the temperature. The temperature is then lowered gradually until the alloy reaches a semisolid state. The blended mixture of preheated SiCp and graphite particles are introduced into the slurry. The SiCp particles help in distributing the graphite particles uniformly throughout the matrix alloy. The temperature during the addition of particles is raised gradually. Stirring is continued until the interface between the particle and the matrix promotes wetting. The casting is finally poured into cast iron permanent molds of 10 mm diameter and 50 mm height. The distribution of SiCp and graphitic particles was studied using optical microscopy and was found to be uniform. Figure 1(a) shows the microstructure of Al/15SiCp/3Gr composite. The SiCp particles are distributed uniformly throughout the matrix alloy. The black regions around SiCp indicate uniform distribution of graphite. The good interfacial bonding between the reinforcing particles and the matrix is evident from Fig. 1(b).

2.2 Experimental Procedure

The aluminum alloy and the composite specimen are tested for its dry sliding wear characteristics using pin on disc test rig as per ASTM G99-95 standard. The dry sliding wear test rig is used to evaluate the wear behavior, as shown in Fig. 2. The wear test conditions are given in Table 2.

The initial weight of the specimen is measured in a single pan electronic weighing machine with an accuracy of 0.0001 gm. After the test, the specimen is cleaned with acetone to remove any debris and then dried. The final mass of the specimen is measured. The mass loss is converted into wear volume loss by using the material's density. Density of the composite is computed using the simple rule of mixtures (Ref 21). Wear rate is obtained by dividing the wear volume loss by the sliding
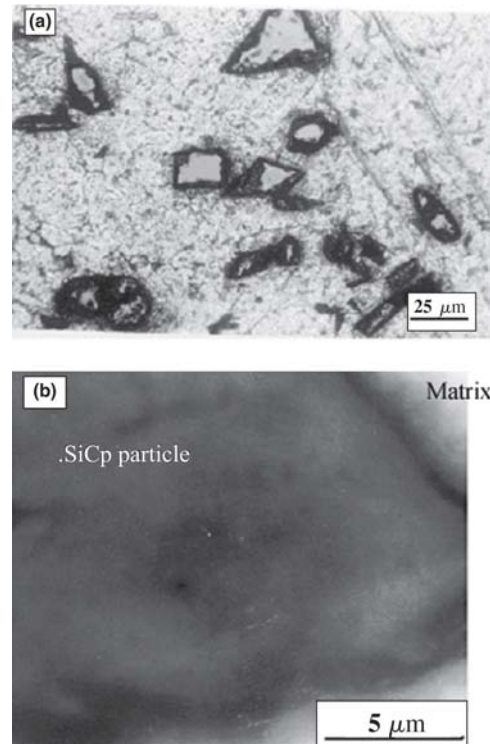

Fig. 1 (a) Microstructure of Al/15SiCp/3Gr, which shows a uniform distribution of the reinforcement particles. (b) Micrograph that shows a good interfacial bond between the matrix and the reinforcing particles.
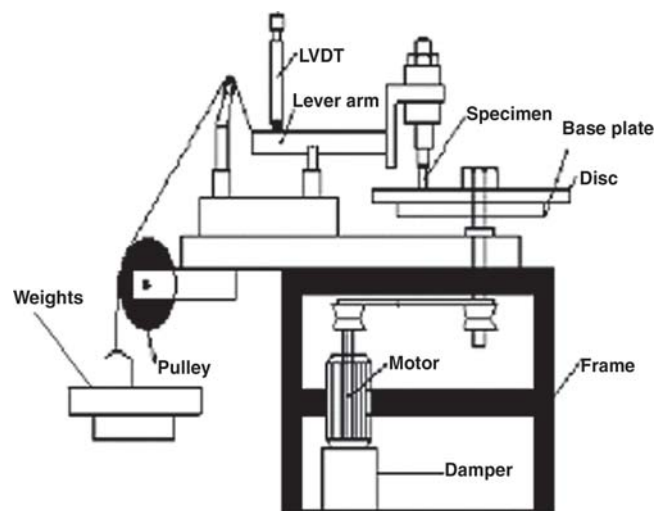

Fig. 2 Schematic diagram of the dry sliding wear testing apparatus

distance. The wear of the composites is studied as a function of the sliding distance, applied load, and the sliding velocity.

3. Experimental Results

3.1 Effect of Sliding Distance and Reinforcement on Wear

Figure 3 shows the variation of dry sliding wear volume loss with sliding distance at an applied load of 40 N and for a

Table 2 Wear test conditions

Pin material	Al 2219, Al 2219/5SiCp/3Gr, Al 2219/10SiCp/3Gr, Al 2219/15SiCp/3Gr
Disc material	EN32 steel disc—65 HRC
Pin contact area	78.5 mm^2
Track radius	114 mm
Sliding speeds	1.53, 3, 4.6, 6.1 m/s
Loads	10-60 N
Relative humidity, %	78%
Temperature	Room temperature (not constant)
Sliding distance	5000 m

Fig. 4   Variation of wear volume against percentage SiCp reinforcement for various sliding distances at 40 N at 4.64 m/s
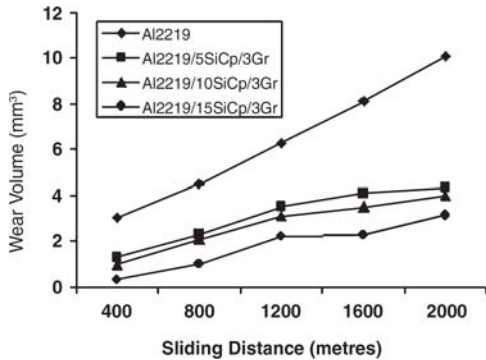
Fig. 3   Variation of wear volume against sliding distance at 40 N at 3 m/s

Fig. 5   Variation of wear rate with sliding speed at constant load of 40 N for a constant sliding distance of 5000 m

sliding speed of 3 m/s. The volume loss of the monolithic alloy and composites increases with the increase in sliding distance. For the base alloy, the wear volume loss increases linearly with the sliding distance. For the composites, the rate of increase in volume loss at long sliding distances decreases. The wear volume loss is less for Al 2219/15SiCp/3Gr compared with other composites and alloy. The effect of SiCp/Gr reinforcement on the wear volume loss of the composites is clearly discerned from Fig. 4 (for a load of 40 N, sliding speed of 4.64 m/s for various sliding distances). The wear resistance of the composites increases with the increase in volume fraction of SiCp reinforcement. The wear resistance of Al 2219/15SiCp/3Gr is the highest among the materials tested. The initial increase in reinforcement content from 0-5%SiCp + 3%Gr decreases the wear volume loss to a maximum extent. With further increase in reinforcement content, the rate of increase of wear resistance is less.

3.2 Effect of Sliding Speed and Load on Wear Rate

The effect of sliding speed on the wear rate is shown in Fig. 5 for the composites and the base alloy for a constant applied load of 40 N and for a constant sliding distance of 5000 m. The wear rate of Al 2219 alloy remains almost constant up to 3 m/s and then increases linearly up to 4.6 m/s. At speeds above 4.6 m/s, the wear rate rapidly increases. For the composites, as the sliding speed increases the wear rate decreases slightly up to 4.6 m/s and then increases. The wear rate is lowest for Al 2219/15SiCp/3Gr composite. The variation of wear rate with applied load at a constant sliding speed of 3 m/s and for a fixed sliding distance of 5000 m is shown in Fig. 6. When the load applied is low, the wear rate is quite small and it increases with the increase in applied load. For Al 2219 alloy, the wear rate
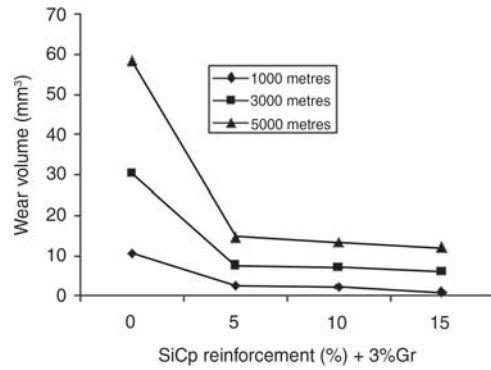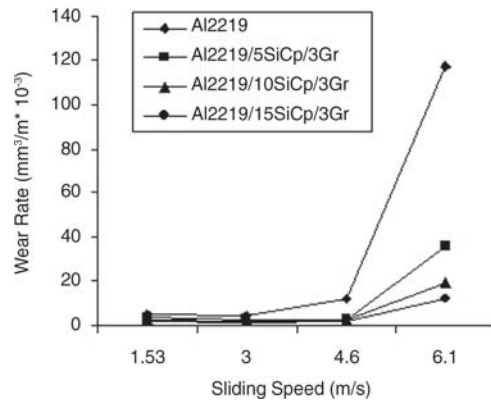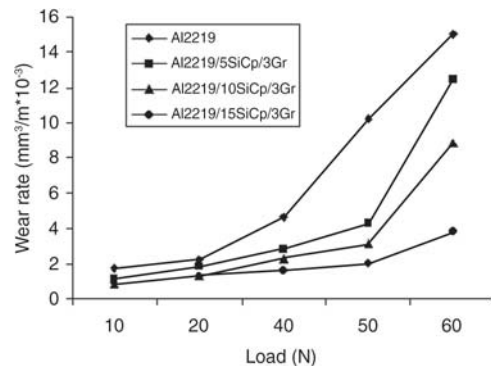

Fig. 6   Variation of wear rate with applied load at a sliding speed of 3 m/s for a sliding distance of 5000 m

increases suddenly (transition load) above 40 N and it enters into a state of severe wear. For the Al 2219/15SiCp/3Gr composite, the severe wear region is not present up to 60 N. The wear rate pattern changes slightly above 50 N.

3.3 Surface Morphology

The entire surface of the pin is in contact with the surface of the counterface during the initial stages of wear. This intact contact between the pin and the counterface results in severe stress on the pin's surface. When sliding starts, the reinforce-
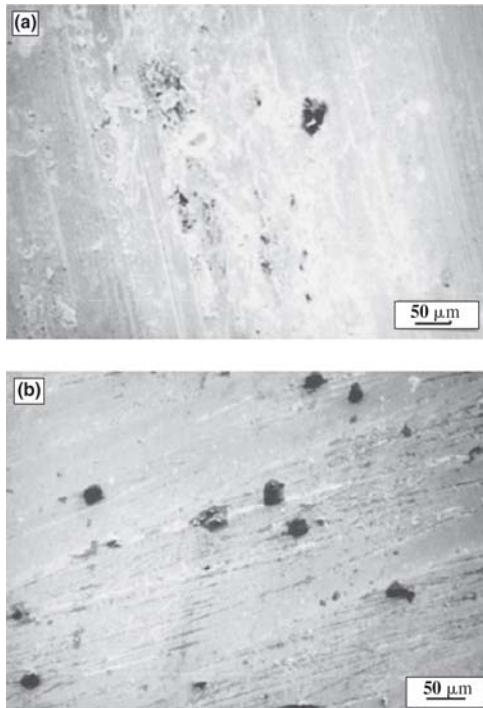
Fig. 7 SEM micrographs of worn surfaces of Al2216/15SiCp/3Gr at 40 N and at a speed of 3 m/s at a sliding distance of (a) 100 m and (b) 500 m
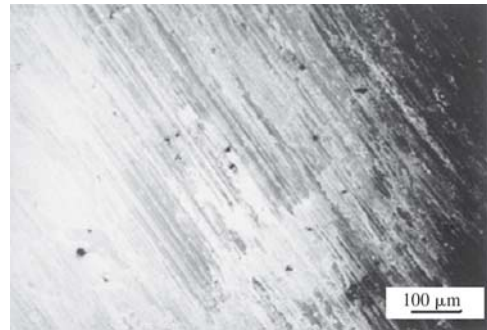

Fig. 8 SEM micrograph of the worn surface at 40 N and at a speed of 3 m/s for a sliding distance of 1500 m
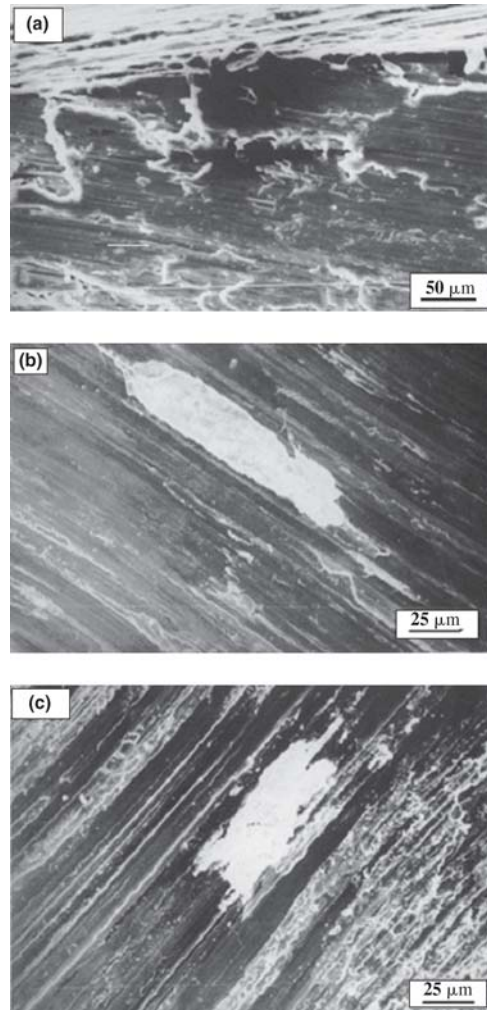

Fig. 9 SEM micrographs of the worn surface at 60 N at a speed of 3 m/s at a sliding distance of 5000 m: (a) Al 2219/5SiCp/3Gr; (b) Al 2219/10SiCp/3Gr; and (c) Al 2219/15SiCp/3Gr composite

ments (SiCp and graphite particles) start to project out from the surface of the pin. Figure 7(a) and (b) shows the micrographs of the worn surfaces of Al 2219/15SiCp/3Gr at an applied load of 40 N and sliding speed of 3 m/s. The micrograph in Fig. 7(a) clearly shows the reinforcements that project out of the surface of the pin after a sliding distance of 100 m. As the sliding distance increases to 500 m, the projecting SiCp start to crack at the leading edges and graphite smears out, as shown in Fig. 7(b).

Figure 8 shows the parallel grooves formed on the surface of the pin after a sliding distance of 1500 m at a sliding speed of 3 m/s and at an applied load of 40 N. These grooves imply that abrasive wear is characterized by the penetration of hard SiCp into the softer surface. At these lower loads and speeds, the fractured particles of SiCp (from the pin) and graphite come between the pin and the counterface. As the load increases to higher values, the morphology of the worn surfaces gradually changes from fine scratches to distinct grooves. The hard particles between the pin and the counterface act as an abrasive medium and ploughs the surface of the pin, causing wear by the removal of small fragments of pin material.

Figure 9(a) to (c) shows the micrographs of the worn surfaces of the composites after a sliding distance of 5000 m at an applied load of 60 N and sliding speed of 3 m/s. For Al 2219/10SiCp/3Gr and Al 2219/15SiCp/3Gr composites, the abrasive ploughs the surface of the pin and the pin material is displaced on to either side of the groove without removing the bulk of the material. This is evident in Fig. 9(b) and (c). In addition, the micrograph clearly shows a layer of material that is removed as debris in the form of thin sheets from the surface. It is considered that this tearing (fracture) causes formation of wear debris. The area of the sheet that is removed from the surface is greater for Al 2219/10SiCp/3Gr than for Al 2219/15SiCp/3Gr.

This confirms the increased wear resistance of Al 2219/15SiCp/3Gr composite.

Figure 9(a) clearly shows the delamination wear of Al 2219/5SiCp/3Gr composite. As the load increases to 60 N, the shear strain induced in the wear process is transmitted to the matrix alloy and the wear mechanism proceeds by subsurface crack propagation causing delamination wear for this composite. Fig-
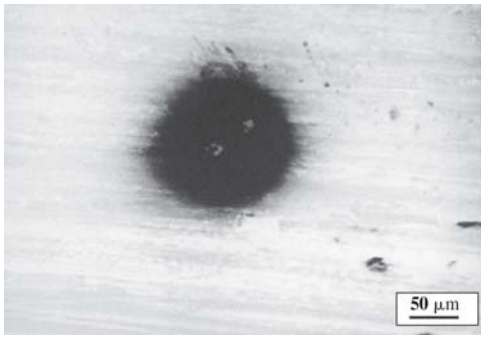
Fig. 10 Micrograph showing the spreading of the graphite on the surface of the pin at 3 m/s speed and 40 N load for Al 2219/10SiCp/3Gr
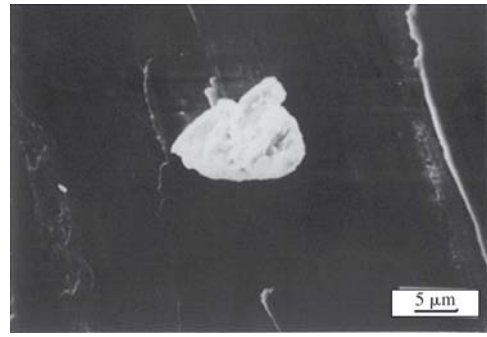

Fig. 11 Micrograph showing the spreading of the graphite on the surface of the pin at 3 m/s speed and 40 N load for Al 2219/10SiCp/3Gr and evidence of the cracking of SiCp

ure 10 shows the spreading of the graphite on the surface of the pin. Figure 11 shows the evidence for the cracking of SiCp. This particle fractures into smaller particles and accumulates between the pin and the counterface reducing wear.

4. Discussion

The volume loss varied with sliding distance as shown in Fig. 3 at a constant sliding speed of 3 m/s and at an applied load of 40 N. For the composites, the rate of increase in wear volume loss is more for sliding distances up to 1200 m. At the start of sliding, the asperities of the pin and the counterface are in contact with each other. Some of the asperities that are not able to resist the shear forces deform, filling the valleys, and parts of the asperities fracture, adding to the wear debris. In addition, the projecting SiCp along with graphite detach itself from the surface of the pin. In this process, the graphite present in the surface of the pin also smears, as shown in Fig. 7(a). As the sliding distance increases, some of the fractured SiCp come between the pin and the counterface and act as an abrasive medium. The fractured bits of SiC plough the surface of the pin causing wear by the removal of small fragments of pin material. The rigidly held SiCp at the surface of the pin wear the steel counterface. Hence, wear increases linearly up to 1200 m.

As sliding distance increases above 1200 m, the SiCp, which are rigidly held to the pin, wears less as compared with the matrix alloy. The ratio of the area of contact of the matrix alloy to that of SiCp against the counterface decreases. Hence, the SiCp take more load compared with the matrix alloy. The hard particles are able to resist wear for a longer time compared with the matrix alloy. Hence, at a sliding distance above 1200 m, the rate of increase of wear decreases. However, for Al 2219 alloy, the wear volume loss increases linearly up to a sliding distance of 2000 m. This agrees well with the general trend of wear behavior as suggested by Archard for monolithic materials (Ref 22).

For the composites, as SiCp reinforcement content increases, the wear decreases, as shown in Fig. 4. This is due to the increase in contact area of SiCp, with the counterface. Hence, the volume loss is less for Al 2219/15SiCp/3Gr compared with other composites.

For the composites, as sliding speed increases, the wear rate decreases up to 4.6 m/s (Fig. 5). When SiCp in the hybrid composites wear the counterface, iron particles from the counterface oxidize forming iron oxides (Fe_2O_3) (Ref 23). Due to the high hardness of the counterface compared with the aluminum base alloy, the fractured SiCp penetrates into the matrix of the composite. However, there is additional SiCp inside the matrix, which will resist the penetration of the SiCp into the matrix alloy (Ref 24). Hence, the SiCp particles are crushed at the interface and powdery SiCp particles are formed. However, at places where graphite particles are present, the SiCp easily penetrate into the matrix alloy due to the low hardness, squeezing some of the graphite from the matrix. The graphite particles smear at the interface and reduce the coefficient of friction. Hence, the heat generated due to friction is also reduced. Figure 10 clearly shows the smearing of graphite at a sliding speed of 3 m/s and an applied load of 40 N.

The powdered SiCp particles along with ferrous oxides from the counterface, aluminum oxides from the pin and graphite are mixed, forming mechanically mixed layer (MML) (Ref 25). The hardness of the MML is much higher than that of the pin and the counterface. This work-hardened layer reduces the wear rate for sliding speeds up to 4.6 m/s. Venketaraman et al. (Ref 25) found that a stable, thin, and hard MML layer formed on the surface of Al 7075/10SiCp composite, increasing the wear resistance of the composite. MML layers form at the interface between the pin and counterface, and hence, separate the wearing surfaces. As SiCp particle (along with graphite) reinforcement content increases, a stable MML layer is formed. Thus, the wear rate of Al 2219/15SiCp/3Gr is less compared with other composite materials tested.

The wear mechanism of Al 2219 alloy at these sliding speeds and loads are different from that of the composites. For Al 2219 alloy, initially at low applied loads up to 20 N and sliding speeds up to 3 m/s (Fig. 5, 6), the wear rate almost remains constant. This is due to the formation of a stable oxide layer. Oxide films are present on almost all metals and form on any clean metal surface exposed to oxygen even at cryogenic temperatures (Ref 26). At sliding speeds between 3 and 4.6 m/s and at loads between 20 and 40 N, the oxide layer would be stable at some points and unstable at other points. The temperature rise causes some of the oxide layer to fracture resulting in lumps of metal being removed (Ref 27). Hence, the wear rate rises in this region of sliding speeds and loads. Sasada et al. (Ref 28) has explained the wear mechanism of metals based on the formation of transfer films at the interface between the sliding surfaces. Transfer films are formed when the Al 2219 pin slides over the steel counterface and they have a dramatic effect on the wear rate (Ref 28). At the beginning of the formation of the transfer layer, the transfer particles are small. As

sliding distance increases, these transfer particles grow bigger and are flattened between the sliding interface of the pin and the counterface producing a lamellar structure. These transfer particles become harder than the alloy due to severe work hardening, and subsequently, plough the surface of the pin (Ref 29). Hence, grooves are formed on the surface of the pin. At sliding speeds up to 4.6 m/s and loads up to 40 N, thick oxide films are formed on the worn surfaces, and hence, 'mild wear' prevails. Above these speeds and loads, the thick oxide films break down and 'severe wear' occurs (Ref 30).

At high sliding speeds above 4.6 m/s, the wear rate pattern of the composites changes. The wear rate increases with the increase in sliding speed. This can be attributed to the rise in interface temperature. At these high-sliding speeds, the hard particles of SiCp and fragments of iron oxide detach from the MML layer and act as third-body abrasives against the steel counterface. Some of the abrasives are trapped in the counterface and wear the aluminum matrix of the composite (Ref 9). Hence, the contact temperature rises and greatly reduces the shear strength of the aluminum facilitating the transfer of softened material to the counterface. The smeared graphite layer slows this temperature rise due to the decrease in friction. The lower coefficient of friction also reduces the shear stresses transferred to the bulk surface material underneath the tribolayer (Ref 9). For this reason, the hybrid composites are able to resist wear for sliding speeds above 4.6 m/s. The wear rate is less for Al 2219/15SiCp/3Gr even at sliding speeds as high as 4.6 m/s. The MML layer formed is stable and able to withstand higher temperatures compared with other materials.

In the severe wear regimen for Al 2219 alloy at speeds above 4.6 m/s and loads greater than 40 N as shown in Fig. 5 and 6, adhesion becomes the predominant wear mechanism (Ref 31). The combined action of adhesion between asperities and sliding motion causes severe plastic deformation of the asperities. Material in the softer, or sharper, asperity deforms in a series of shear bands (Ref 32). When each shear band reaches a certain limit, a crack is initiated, or an existing crack propagates, until a new shear band is formed. The crack extends across the asperity and eventually a particle detaches from the deformed asperity (Ref 21, 32).

The wear rate increases at a faster rate after the load exceeds 50 N for the Al 2219/5SiCp/3Gr composite (Fig. 6). The mechanism controlling the wear process is delamination (Ref 33). Plastic deformation occurs due to the surface traction exerted on the surface of the composite. Cracks cannot nucleate very near the surface due to the large hydrostatic pressure that exists right beneath asperity contact (Ref 33). As the subsurface deformation continues, cracks nucleate below the surface. Once the cracks are present further loading and deformation causes the cracks to extend and propagate, eventually joining with neighboring cracks. The subsurface cracks also propagate along the particle matrix interface, causing particle-matrix decohesion (Ref 34). When the cracks finally shear the surface, long and thin sheets delaminate (Ref 33). The micrograph in Fig. 9(a) shows the material removed in the form of thin sheets from the surface of Al 2219/5SiCp/3Gr composite due to delamination. The thickness of the wear sheet is determined by the location and growth of subsurface cracks.

5. Conclusions

Dry sliding wear of Al 2219/SiCp/Gr composites and Al 2219 alloy has been investigated under a broad range of sliding speeds and loads. Addition of graphite to the Al/SiCp composite increases the wear resistance of the composites by smearing a graphite layer at the interface between the pin and the counterface. The reinforcements reduce the wear rate and increase the transition load from mild to severe wear. As sliding speed and load increase, a MML layer is formed that reduces wear. Wear resistance is highest for Al/15SiCp/3Gr. For the composites, wear is by abrasion at low sliding speeds and loads, changing to delamination at high loads, which occurs due to subsurface crack propagation.

References

1. S. Suresh, A. Mortensen, and A. Needleman, *Fundamentals of Metal Matrix Composites,* Stoneham, Butterworth-Heinemann, 1993

2. M. Taya and R.J. Arsenault, *Metal Matrix Composites—Thermo Mechanical Behavior,* New York, Pergamon Press, 1989

3. A. Ibrahim, F.A. Mohammed, and E.J. Lavernia, Metal Matrix Composites—A review, *J. Mater. Sci.,* 1991, **26,** p 1137-1157

4. A.P. Sannino and H.J. Rack, Dry Sliding Wear of Discontinuously Reinforced Aluminum Composites—Results and Discussions, *Wear,* 1995, **189,** p 1-19

5. R.L. Deuis, C. Subramanian, and J.M. Yellup, Abrasive Wear of Aluminum Composites—A Review, *Wear,* 1996, **201,** p 132-144

6. J. Goni, Development of Low Cost Metal Matrix Composites for Commercial Applications, *Mater. Sci. Technol.,* 2000, **16,** p 743-746

7. G.J. Howell and A. Ball, Dry Sliding Wear of Particulate Reinforced Al Alloys against Automobile Friction Materials, *Wear,* 1995, **181-183,** p 379-390

8. G. Straffelini, M. Pellizzari, and A. Molinari, Influence of Load & Temperature on the Dry Sliding Behavior of Aluminum Based Metal Matrix Composites against Frictional Material, *Wear,* 2004, **256,** p 754-763

9. A.R. Riahi and A.T. Alpas, The Role of Tribo Layers on the Sliding Wear Behavior of Graphite MMC, *Wear,* 2001, **251,** p 1396-1407

10. T. Ma, H. Yamaura, D.A. Koss, and R.C. Voigt, Dry Sliding Wear Behavior of Cast SiCp Reinforced Al MMC's, *Mater. Sci. Eng.,* 2003, **A360,** p 116-125

11. S. Kassim and Al-Rubaie, Three Body Abrasion of Al-SiCp Composites, *Wear,* 1999, **225-229,** p 163-173

12. K.H.W. Seah, S.C. Sharma, B.M. Girish, and S.C. Lim, Wear Characteristics of as Cast Za-27/Graphite Particulate Composites, *Mater. Des.,* 1996, **17**(2), p 63-67

13. S. Mohan, J.P. Pathak, R.C. Gupta, and S. Srivastava, Wear Behavior of Graphitic Al Composite Sliding under Dry Conditions, *Z. Metallkd,* 2002, **93**(12), p 1245-1251

14. Y. Zhan and G. Zhang, The Role of Graphite Particles in the High Temperature Wear of Copper Hybrid Composites Against Steel, *Mater. Des.,* 2006, **27,** p 79-84

15. S. Das, S.V. Prasad, and T.R. Ramachandran, Microstructure and Wear of Cast Al-Si Alloy Graphite Composites, *Wear,* 1989, **133,** p 173-187

16. S.K. Rhee, Friction Coefficient of Automotive Friction Materials—Its Sensitivity to Load, Speed and Temperature, *SAE Trans.,* paper 740415, 1974

17. P.K. Rohatgi, S. Ray, and Y. Liu, Tribological Properties of Metal Matrix-Graphite Particle Composites, *Int. Mat. Rev.,* 1992, **37,** p 129-149

18. J.R. Davis, *ASM Specialty Handbook,* ASM*,* 1993

19. S.C. Sharma, B.M. Girish, D.R. Somashekar, B.M. Satish, and R. Kamath, Sliding Wear Behavior of Zircon Particles Reinforced ZA-27 Alloy Composite Materials, *Wear,* 1999, **224,** p 89-94

20. S.C. Sharma, The Sliding Wear Behavior of Al6061-Garnet Particulate Composites, *Wear,* 2001, **249,** p 1036-1045

21. V. Constantin, L. Scheed, and J. Masounave, Sliding Wear of Aluminum-Silicon Carbide Metal Matrix Composites, *ASME-Journal of Tribology,* 1999, **121,** p 787-794

22. J.F. Archard, Contact and Rubbing of Flat Surfaces, *J. Appl. Phys.,* 1953, **24,** p 981-985
23. J. Glascott, G.F. Wood, and F.H. Stott, The Influence of Experimental Variables on the Development and Maintenance of Wear-Protective Oxides during Sliding of High-Temperature Iron-Base Alloys, *Proc. Inst. Mech. Engrs.,* Vol. 199, pt.C, 1985, p 35-41
24. Y. Sahin, Wear Behavior of Aluminum Alloy and Its Composites Reinforced by SiC Particles Using Statistical Analysis, *Mater. Des.,* 2003, **24,** p 95-103
25. B. Venkataraman and G. Sundararajan, Correlation between the Characteristics of the Mechanically Mixed Layer and Wear Behavior of Aluminum, Al-7075 Alloy and Al-MMCs, *Wear,* 2000, **245,** p 22-38
26. N.D. Tomashow, *Theory of Corrosion and Protection of Metals*, New York, McMillan, 1966
27. R. Colas, J. Ramrez, I. Sandoval, J.C. Morales, and L.A. Leduc, Damage in Hot Rolling Work Rolls, *Wear,* 1999, **230,** p 56-60
28. T. Sasada, S. Norose, and H. Mishina, The Behavior of Adhered Fragments Interposed between Sliding Surfaces and the Formation Process of Wear Particles, *Proc. Int. Conf. on Wear of Materials,* ASME, 1979, p 72-80
29. K. Komvopoulos, N. Saka, and N.P. Suh, The Mechanism of Friction in Boundary Lubrication, *ASME-Journal of Tribology,* 1985, **107,** p 452-463
30. J.F. Archard and W. Hirst, The Wear of Metals Under Unlubricated Conditions, *Proc. Roy. Soc.,* Series A, Vol 236, 1956, p 397-410
31. J.F. Archard, Single Contacts and Multiple Encounters, *J. Appl. Phys.,* 1961, **32,** p 1420-1425
32. T. Kayaba and K. Kato, The Analysis of Adhesive Wear Mechanism by Successive Observations of the Wear Process in SEM, *Proc. Int. Conf. on Wear of Materials,* ASME, 1979, p 45-46
33. N.P. Suh, *Tribophysics,* Prentice Hall, Englewood Cliffs, NJ, 1986.
34. A.T. Alpas and J. Zhang, Effect of Microstructure and Counterface Material on the Sliding Wear Resistance of Particulate Reinforced Aluminum Matrix Composites, *Metall. Trans. A,* 1994, **25,** p 969-983